ELSEVIER

Chemical Geology 200 (2003) 105–115

CHEMICAL GEOLOGY
INCLUDING
ISOTOPE GEOSCIENCE

www.elsevier.com/locate/chemgeo

Modelling molybdate and tungstate adsorption to ferrihydrite

Jon Petter Gustafsson*

Department of Land and Water Resources Engineering, Royal Institute of Technology, KTH, SE-100 44, Stockholm, Sweden

Received 7 November 2002; accepted 9 April 2003

Abstract

The environmental geochemistry of molybdenum and tungsten is not well known. To enable predictions of Mo and W concentrations in the presence of ferrihydrite (hydrous ferric oxide), batch equilibrations were made with MoO_4^{2-}, WO_4^{2-}, *o*-phosphate (PO_4^{3-}) and freshly prepared ferrihydrite suspensions in 0.01 M $NaNO_3$ in the pH range from 3 to 10 at 25 °C. The results showed that WO_4^{2-} is adsorbed more strongly than MoO_4^{2-}, and that both ions are able to displace PO_4^{3-} from adsorption sites at low pH. Two models, the Diffuse Layer Model (DLM) and the CD-MUSIC Model (CDM), were tested in an effort to describe the data. In both models, the adsorption of MoO_4^{2-} and WO_4^{2-} could be described with the use of two monodentate complexes. One of these was a fully protonated complex, equivalent to adsorbed molybdic or tungstic acid, which was required to fit the data at low pH. This was found to be the case also for a data set with goethite. In competitive systems with PO_4^{3-}, the models did not always provide satisfactory predictions. It was suggested that this may be partly due to the uncertainty in the PO_4^{3-} complexation constants.

Keywords: Molybdenum; Tungsten; Hydrous ferric oxide; Surface complexation; Modelling

1. Introduction

Molybdenum is an essential trace element for both plants and animals. Molybdenum deficiency has often been reported, but at large concentrations, Mo may be toxic as it leads to secondary Cu deficiency (e.g., Vunkova-Radeva et al., 1988). Of particular concern is the release of Mo from alkaline ashes when used as secondary materials (Jacks, 1983; Meima et al., 2002). Tungsten is an important strategic metal that is used in a variety of industrial applications. It is usually mined from deposits of scheelite ($CaWO_4$) and wolframite ($(Fe,Mn)WO_4$. Tungsten is released to the environment, e.g., through its use in winter tires. The biogeochemical behaviour of W is poorly known. However, it is known that the WO_4^{2-} ion has an antagonistic effect on the metabolism of MoO_4^{2-} (Mikkonen and Tummavuori, 1993).

At relatively high Eh, Mo and W are present in their hexavalent state, i.e., as MoO_4^{2-} and WO_4^{2-}, and their derivatives. From equilibrium modelling, it can be predicted that the fully dissociated MoO_4^{2-} and WO_4^{2-} ions predominate over the non-dissociated forms at pH>4.4 in dilute waters (Cruywagen, 2000; Smith et al., 2001). At pH < 4.4, the ions will protonate to form the acids $MoO_3(H_2O)_3$ and $WO_3(H_2O)_3$, in which Mo and W coordinate six oxygens instead of four. At large concentrations (>1–10 μM), Mo and W polymerise to a variety of different polymolybdate/tungstate forms,

* Fax: +46-8-411-0775.
E-mail address: gustafjp@kth.se (J.P. Gustafsson).

0009-2541/03/$ - see front matter © 2003 Elsevier Science B.V. All rights reserved.
doi:10.1016/S0009-2541(03)00161-X

particularly at low pH (Cruywagen, 2000). In solution, a wide range of complexes with organic acids has been reported (e.g., Cruywagen et al., 1995).

The geochemical behaviour of MoO_4^{2-} and WO_4^{2-} in the environment is probably dependent, to a large extent, on adsorption reactions to particle surfaces. In soils, it is found that these ions were bound most strongly at low pH (Mikkonen and Tummavuori, 1993, 1994; Bibak and Borggaard, 1994).

Iron, aluminium and, to some extent, titanium oxides may be important sorbent minerals for MoO_4^{2-} and WO_4^{2-}, as they may acquire positive charge at low pH (Bibak and Borggaard, 1994; Rietra et al., 1999; Bourikas et al., 2001). The binding mechanism to these oxides is thought to be surface complexation, either as mono- or bidentate complexes (e.g., Manning and Goldberg, 1996; Bourikas et al., 2001). Goldberg et al. studied the adsorption of molybdate onto goethite, gibbsite and clay minerals (e.g., Goldberg et al., 1996; Manning and Goldberg, 1996; Goldberg and Forster, 1998). They found that adsorption is very strong at low pH; in this pH region, molybdate is able to compete well even with the very strongly sorbing *o*-phosphate (PO_4^{3-}) ion. However, molybdate adsorption exhibited a very strong pH dependence, and at pH>9, little Mo was adsorbed. These authors used a surface complexation model, the Constant Capacitance Model (CCM), to describe the data obtained with the use of two Mo surface complexes.

For the adsorption of MoO_4^{2-} to two-line ferrihydrite (hydrous ferric oxide), data sets are rather sparse. Two exceptions are small data sets published by Balistrieri and Chao (1990) and Bibak and Borggaard (1994), which follow the general trend described above for goethite. No data set has been found that treats the adsorption of WO_4^{2-} to ferrihydrite. In their compilation of constants for the Diffuse Layer Model (DLM), Dzombak and Morel (1990) did not fit any data sets for MoO_4^{2-} and WO_4^{2-}; instead, they estimated constants using linear-free energy relationships (LFER).

A third surface complexation model is CD-MUSIC (Hiemstra and Van Riemsdijk, 1996), which was used to describe MoO_4^{2-} adsorption to titania (Bourikas et al., 2001). Their model suggested MoO_4^{2-} adsorption to be dominated by a bidentate complex at low pH ($Ti_2O_2MoO_2$) and by a monodentate complex ($TiMoO_3$) at high pH. In line with this, Rietra et al. (1999) suggested a bidentate complex ($Fe_2O_2MoO_2$) to dominate the speciation of adsorbed Mo to goethite, as judged from measurements of the proton coadsorption stoichiometry at pH 4.2 and 6.1.

The objectives of this study were to supply data on the adsorption of MoO_4^{2-} and WO_4^{2-} to two-line ferrihydrite at different pHs and surface coverages, to discuss the effect of competing PO_4^{3-} ions, and to apply two surface complexation models (DLM and CD-MUSIC) in an effort to describe the data obtained. To my knowledge, this is the first time that the adsorption of WO_4^{2-} to ferrihydrite has been studied in this manner. For the DLM, it was hypothesized that the constants previously estimated from LFER could describe the data accurately.

2. Methods

2.1. Laboratory procedures

Ferrihydrite was synthesized using a method adapted from Swedlund and Webster (1999) and Schwertmann and Cornell (2000). Briefly, a solution containing 36 mM $Fe(NO_3)_3$ and 12 mM $NaNO_3$ was brought to pH 8.0 through dropwise addition of 4 M NaOH. The resulting suspension was aged for 18–22 h at 20 °C. This procedure has been shown to produce two-line ferrihydrite with a BET(N_2) surface area in the range of 200–320 $m^2\ g^{-1}$ (Swedlund and Webster, 1999; Schwertmann and Cornell, 2000). However, the exact value is strongly dependent on the outgassing conditions, which are seldom reported (Clausen and Fabricius, 2000). Moreover, it is believed that the BET(N_2) method underestimates the real surface area of ferrihydrite considerably, probably because of aggregation of nanoparticles, which makes part if the surface inaccessible to the N_2 sorbate (Dzombak and Morel, 1990; Schwertmann and Cornell, 2000). For these reasons, BET surface areas are of limited interest for the characterization of two-line ferrihydrite, and they can probably not be used for modelling purposes. Hence, they were not measured. Instead, surface areas of 600 and 750 $m^2\ g^{-1}$ was assumed for the 2-p*K* DLM (Dzombak and Morel, 1990; Swedlund and Webster, 1999) and for the 1-p*K* CD-MUSIC Model (CDM) (Gustafsson, 2001), respectively (see below). These areas are in better agreement with the surface area inferred from

Table 1
Table of species for adsorption reactions in the DLM and values of log K_{int}^{a}

Species	P_o^b	FeOH	H^+	MoO_4^{2-}	WO_4^{2-}	PO_4^{3-}	log K_{int} (Dzombak and Morel, 1990)	log K_{int} (this study)
D1. $FeOMo(OH)_5$	0	1	2	1	0	0	–	17.96
D2. $FeOMoO_3^-$	−1	1	1	1	0	0	9.5[c]	–
D3. $FeOHMoO_4^{-2}$	−2	1	0	1	0	0	2.4[c]	3.14
D4. $FeOW(OH)_5$	0	1	2	0	1	0	–	19.31
D5. $FeOWO_3^{-1}$	−1	1	1	0	1	0	9.2[c]	–
D6. $FeOHWO_4^{-2}$	−2	1	0	0	1	0	2.1[c]	6.4
D7. $FeOPO_3H_2$	0	1	3	0	0	1	31.29	32.08
D8. $FeOPO_3H^{-1}$	−1	1	2	0	0	1	25.39	26.39
D9. $FeOPO_3^{-2}$	−2	1	1	0	0	1	17.72	20.73

[a] Water molecules are not included in the table of species.
[b] $P_o = \exp(-F\Psi_o/RT)$, where F is the Faraday constant, Ψ_o is the electrostatic potential in the o-plane, R is the gas constant and T is the absolute temperature.
[c] These values were estimated from linear free-energy relationships only.

theoretical grounds (Dzombak and Morel, 1990; Schwertmann and Cornell, 2000).

Before the batch experiments, the ferrihydrite suspension was back-titrated to pH 4.6 with 0.1 M HNO_3 and vigorously shaken for 15 min. Batch experiment suspensions was prepared by mixing an amount of ferrihydrite suspension with stock solutions of $NaNO_3$ and the appropriate anion salt (as Na_2MoO_4, Na_2WO_4 or NaH_2PO_4) to obtain suspensions with an ionic strength of 0.01 M (as $NaNO_3$). Various amounts of acid (as HNO_3) or base (as NaOH) was added to produce a range of pHs. In the single-sorbate systems, only one anion (except NO_3^-) was added at concentrations of 50 μM MoO_4^{2-}, 50 μM WO_4^{2-} or 200 μM PO_4^{3-}; in these systems, anion sorption was studied at three different concentrations of ferrihydrite, which contained 0.3, 1 and 3 mM total Fe (however, there was no PO_4^{3-} system with 0.3 mM Fe). In the binary (competitive) systems, the ferrihydrite concentration was 1 mM as total Fe, whereas the anion concentrations were either 50 μM MoO_4^{2-} + 200 μM PO_4^{3-} or 50 μM WO_4^{2-} + 200 μM PO_4^{3-}. The samples were equilibrated in 40 ml polypropylene centrifuge tubes.

After 24 h of equilibration in a shaking water bath at 25 °C, the samples were centrifuged for 30 min at about 5000 × g and filtered using 0.2-μm single-use filters (Acrodisc PF). The pH was measured on the unfiltered sample, using a radiometer combination electrode. The filtered suspension was acidified (0.5% HNO_3) and analysed for W, Mo and P with plasma emission spectroscopy using a Jobin-Yvon JY24 ICP instrument. Preliminary experiments with WO_4^{2-} spikes in acidified solutions in polypropylene containers showed that the WO_4^{2-} concentration started to decrease after a few

Table 2
Table of species for adsorption reactions in the CDM and values of log K_{int}^{a}

Species	P_o^b	P_b^b	FeOH	H^+	MoO_4^{2-}	WO_4^{2-}	PO_4^{3-}	log K_{int} (Gustafsson, 2001)	log K_{int} (this study)
C1. $FeOMo(OH)_5^{-0.5}$	0.5	−0.5	1	2	1	0	0	–	18.28
C2. $FeOMoO_3^{-1.5}$	0.5	−1.5	1	1	1	0	0	–	11.17
C3. $FeOW(OH)_5^{-0.5}$	0.5	−0.5	1	2	0	1	0	–	19.35
C4. $FeOWO_3^{-1.5}$	0.5	−1.5	1	1	0	1	0	–	14.07
C5. $FeOPO_3H_2^{-0.5}$	0.5[c]	−0.5[c]	1	3	0	0	1	32.1	31.53
C6. $Fe_2O_2POOH^{-1}$	1	−1	2	3	0	0	1	35.6	34.13
C7. $Fe_2O_2PO_2^{-2}$	0.5	−1.5	2	2	0	0	1	29.0	26.64

[a] Water molecules are not included in the table of species.
[b] $P_o = \exp(-F\Psi_o/RT)$ and $P_b = \exp(-F\Psi_b/RT)$, where F is the Faraday constant, Ψ_o and Ψ_b are electrostatic potentials in the o- and b-planes, R is the gas constant and T is the absolute temperature.
[c] The P_o and P_b values of this complex were previously set to 0.8 and −0.8 (Gustafsson, 2001), but they were revised in this study.

Table 3
Measured pH and dissolved concentrations of MoO_4, WO_4 and PO_4 in the batch experiments

MoO_4 added			WO_4 added		
Total Fe (M)	pH	MoO_4^{2-} (μM)	Total Fe (M)	pH	WO_4^{2-} (μM)
3×10^{-3}	3.13	<0.1	3×10^{-3}	3.14	<0.1
	3.64			3.65	
	5.20			5.23	
	5.94			5.94	
	6.30	0.15		6.42	
	6.59	0.63		6.66	
	6.87	3.15		6.94	
	7.07	7.7		7.34	0.3
	7.20	13.4		7.73	1.1
	7.21	19.5		8.46	2.8
	7.71	26.2		8.75	5.8
	7.85	31.6		8.86	7.7
	8.30	36.0		9.06	11.4
	8.46	38.8		9.24	14
	8.81	42.5		9.37	17
	9.76	47.5		9.83	27
1×10^{-3}	3.11	<0.1	1×10^{-3}	3.11	
	3.64			3.65	<0.1
	6.39	1.45		6.43	
	6.91	9.26		7.29	1.7
	7.09	15.4		7.55	5.8
	7.23	20.4		7.81	10.1
	7.29	25.7		8.24	16.2
	7.44	32.0		8.38	19.6
	7.71	38.2		8.74	24.2
	7.89	40.3		8.94	27.8
	8.39	44.4		9.09	31.1
3×10^{-4}	3.09	1.05	3×10^{-4}	3.10	<0.1
	3.65	0.72		3.65	
	6.06	19.5		6.54	12.6
	6.66	27.5		7.02	21.9
	6.83	33.2		7.30	26.6
	7.01	35.2		7.41	29.1
	7.13	39.4		7.66	34.0
	7.20	40.4		7.90	36.7
	7.28	44.6		8.15	36.4
	7.55	45.6		8.31	38.7
	8.53	48.9		8.97	41.0
	9.08	48.1		9.12	43.4

PO_4 added					
Total Fe (M)	pH	PO_4^{3-} (μM)	Total Fe (M)	pH	PO_4^{3-} (μM)
3×10^{-3}	3.10	<1	1×10^{-3}	3.10	2
	3.60			3.68	6
	4.12			4.68	24
	4.26			5.23	39
	4.44			5.85	56
	4.70			6.26	69

Table 3 (*continued*)

PO_4 added					
Total Fe (M)	pH	PO_4^{3-} (μM)	Total Fe (M)	pH	PO_4^{3-} (μM)
	5.07			6.45	71
	5.70			6.62	82
	6.39			6.94	92
	6.82	1		7.18	98
	7.49	11		7.48	108
	8.06	28		7.73	120

$PO_4 + MoO_4$ added, 1×10^{-3} M total Fe			$PO_4 + WO_4$ added, 1×10^{-3} M total Fe		
pH	PO_4^{3-} (μM)	MoO_4^{2-} (μM)	pH	PO_4^{3-} (μM)	WO_4^{2-} (μM)
3.13	14	1.28	3.14	11	<0.1
3.83	35	1.92	3.84	31	
4.63	56	4.6	4.68	54	
4.97	58	8.84	5.16	69	0.8
5.36	63	17.5	5.67	81	2.9
5.74	71	26.6	6.10	93	5.9
6.08	77	34.6	6.42	99	10.9
6.40	79	41.4	6.66	104	16.6
6.69	80	41.9	6.89	100	19.3
6.94	86	46.3	7.11	102	22.5
7.2	89	46.7	7.32	111	29.0
7.45	104	49.3	7.55	116	33.1

days, probably because of the formation of an insoluble surface phase on the container walls. To avoid this, analysis was carried out within 24 h of filtration, to avoid the risk for WO_4^{2-} loss from solution due to its slow adsorption to the container walls.

2.2. Modelling

The surface complexation models used were the 2-p*K* DLM (according to Dzombak and Morel, 1990) and the 1-p*K* CDM with the Three-Plane interface model (Hiemstra and Van Riemsdijk, 1996, 1999). I used the same DLM parameters as Dzombak and Morel (1990): a specific surface area of 600 $m^2\ g^{-1}$ was assumed, the site density was fixed at 0.205 mol mol^{-1} Fe, and the log *K*'s of the surface complexation reactions defining the formation of the protonated $FeOH_2^+$ species and the deprotonated FeO^- species were set at 7.29 and −8.93, respectively. Table 1 shows the surface complexation reactions involving Mo, W and P.

For the CDM, I used the surface charging parameters as was suggested in an earlier study (Gustafsson,

2001): a specific surface area of 750 $m^2\ g^{-1}$, a site density of 0.443 mol mol^{-1} Fe of singly coordinated FeOH groups, a log K for the formation of $FeOH_2^{1/2+}$ of 8.1, log K's for the ion-pair complexes $FeOHNa^{1/2+}$ and $FeOH_2NO_3^{1/2-}$ of −0.4 and 7.2, respectively, an inner capacitance of 1.3 F m^{-2} and an outer capacitance of 5 F m^{-2}. Table 2 lists the other surface complexation reactions considered.

In the modelling, I considered the protonation reactions of the MoO_4^{2-} and WO_4^{2-} ions:

$$H^+ + XO_4^{2-} \leftrightarrow HXO_4^-,\ K_1 \quad (1)$$

$$2H^+ + XO_4^{2-} + 2H_2O \leftrightarrow XO_3(H_2O)_3,\ K_2 \quad (2)$$

Here, X is Mo or W, whereas K_1 and K_2 are equilibrium constants. For Mo, log K_1 and log K_2 were set to 4.24 and 8.24, respectively, using the most recent NIST reference database values (Smith et al., 2001). For W, I used log $K_1 = 3.62$ (Wesolowski et al., 1984), whereas log $K_2 = 8.7$ was estimated from extrapolation of data obtained by Wood and Samson (2000) to room temperature. The model fits was not sensitive to the exact value of these constants, as most data were collected at pH>5. Polymeric Mo and W species were considered using the 1 M constants compiled by Cruywagen (2000), which had been extrapolated to 0 M ionic strength using the Davies equation. However, the polymeric species were found to be insignificant in this study.

The chemical equilibrium program Visual MINTEQ (Gustafsson, http://www.lwr.kth.se/English/OurSoftware/vminteq/index.htm) was used to produce model fits with previously determined surface complexation constants. To optimise new surface complexation constants, FITEQL 4.0 was used (Herbelin and Westall, 1999), which is a non-linear least-squares optimisation program. In the standard version, FITEQL 4.0 contains the DLM, but not the CDM. Therefore, to deal with the results from this study, FITEQL 4.0 was modified to include the Three-Plane interface model and to permit the non-zero charge of the reference oxide component, as required by the 1-pK CDM. In addition, the constants of multidentate surface species were redefined on a mole fraction basis (Hiemstra and Van Riemsdijk, 1996). Obtained equilibrium constants were averaged using the weighting method of Dzombak and Morel (1990), in which the weighting factor w_i is defined as

$$w_i = \frac{(1/\sigma_{\log K})_i}{\Sigma(1/\sigma_{\log K})_i} \quad (3)$$

where $(\sigma_{\log K})_i$ is the standard deviation of log K calculated by FITEQL for the ith data set. The best estimate for log K is then calculated as:

$$\overline{\log K} = \Sigma w_i (\log K)_i. \quad (4)$$

3. Results

3.1. Single-sorbate systems

A detailed account of the results obtained can be found in Table 3. Molybdate adsorption was strongly

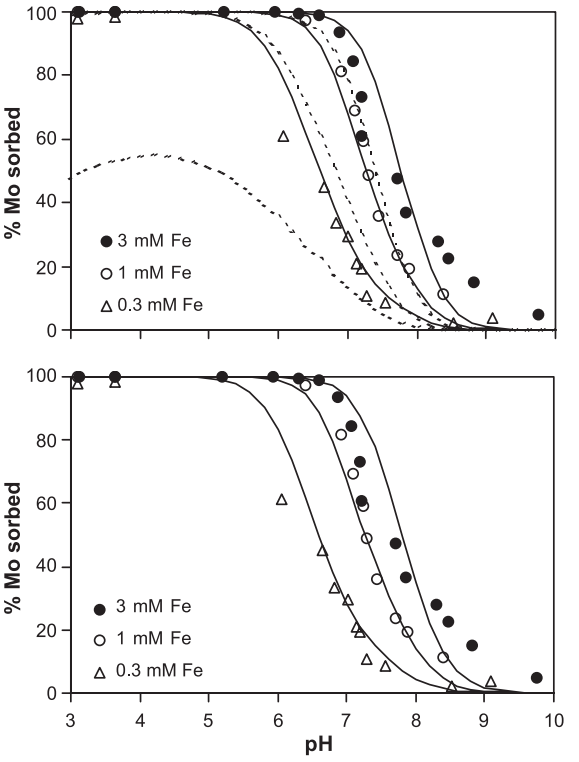

Fig. 1. Adsorption of molybdate (50 μM added) to ferrihydrite in single-sorbate systems. Points are observations, and lines are fits with the DLM (upper panel) or CDM (lower panel). The dotted line is the model fit obtained with the non-optimised constants in Tables 1 and 2, whereas the solid line represents the fit obtained with the weighted average constants in Tables 4 and 5.

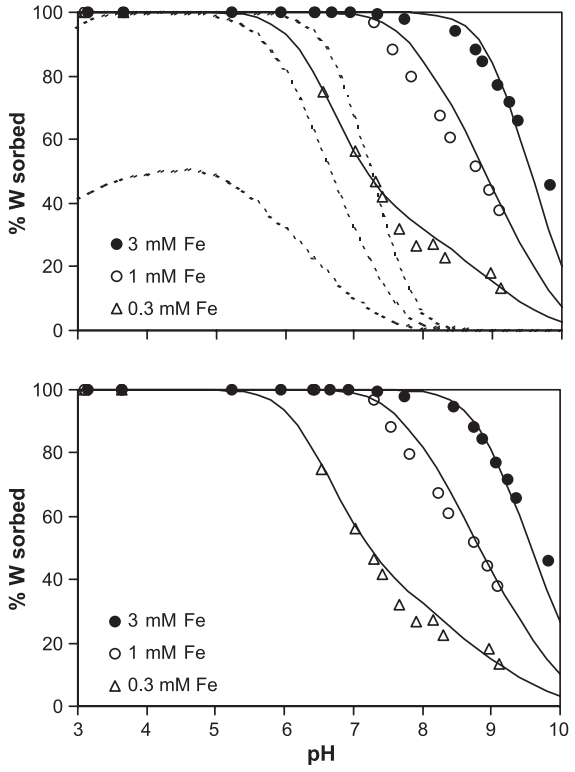

Fig. 2. Adsorption of tungstate (50 μM added) to ferrihydrite in single-sorbate systems. Points are observations, and lines are fits with the DLM (upper panel) and the CDM (lower panel). The dotted line is the model fit obtained with the non-optimized constants in Tables 1 and 2, whereas the solid line represents the fit obtained with the weighted average constants in Tables 4 and 5.

pH dependent (Fig. 1, Table 3), which is consistent with earlier studies. Even at the highest surface coverage (0.3 mM Fe), almost 100% was adsorbed at low pH, whereas little Mo adsorption occurred at pH>9 at all surface coverages. For MoO_4^{2-}, there was considerable scatter in the adsorption envelopes. It is possible that errors in pH measurements may, in part, explain this, as most pH values were in the circumneutral region (pH 6–8), where the ferrihydrite suspensions were extremely poorly buffered.

Tungstate adsorption was also strongly pH dependent (Fig. 2, Table 3). At low surface coverage, the adsorption envelopes were shifted almost 2 pH units upwards compared with molybdate, which shows that WO_4^{2-} was adsorbed much more strongly than MoO_4^{2-} to ferrihydrite. The higher pH probably explains the smaller degree of scatter in the WO_4^{2-} adsorption envelopes.

When Dzombak and Morel's DLM constants for MoO_4^{2-} (as estimated by LFER) were used (Table 1), I found that the adsorption of MoO_4^{2-} was underestimated slightly at the two lower surface coverages (Fig. 1, dotted lines). At the highest surface coverage, the constants were quite unable to describe the near 100% adsorption occurring at low pH. To improve the DLM description of MoO_4^{2-} binding, a fully protonated species D1 had to be included in the model; this is referred to as $FeOMo(OH)_5$ in Table 1 and may be thought of as adsorbed molybdic acid. The FITEQL optimisation led to reasonable results either with a combination of species D1 and D3, or with a combination of species D1 and D2. Of these combinations, the former was chosen because a slightly better fit was obtained. Table 4 shows the optimisation results and the solid line of Fig. 1 the actual fit (solid line).

For WO_4^{2-}, Dzombak and Morel's LFER constants severely underestimated the adsorption at all surface

Table 4
Intrinsic DLM adsorption constants (standard deviations in parenthesis) from experimental data for molybdate and tungstate adsorption to ferrihydrite[a]

Molybdate

Total Fe (M)	log K_{D1}^{INT}	log K_{D3}^{INT}	WSOS/DF
3×10^{-3}	17.96[b]	3.05 (0.039)	23
1×10^{-3}	18.28 (0.087)	3.19 (0.092)	3.4
3×10^{-4}	17.73 (0.063)	3.37 (0.13)	3.7
Weighted average	17.96	3.14	

Tungstate

Total Fe (M)	log K_{D4}^{INT}	log K_{D6}^{INT}	WSOS/DF
3×10^{-3}	19.31[b]	6.60 (0.037)	4.9
1×10^{-3}	19.31[b]	6.21 (0.046)	2.5
3×10^{-4}	19.31 (0.064)	6.24 (0.13)	1.7
Weighted average	19.31	6.40	

Phosphate

Total Fe (M)	log K_{D7}^{INT}	log K_{D8}^{INT}	log K_{D9}^{INT}	WSOS/DF
1×10^{-3}	32.08 (0.18)	26.39 (0.29)	20.73 (0.60)	2.7

[a] The method of Dzombak and Morel (1990) was used to obtain error estimates and weighted averages.
[b] Fixed at this value to achieve convergence.

Table 5
Intrinsic CDM adsorption constants (standard deviations in parenthesis) from experimental data for molybdate and tungstate adsorption to ferrihydrite[a]

Molybdate

Total Fe (M)	log K_{C1}^{INT}	log K_{C2}^{INT}	WSOS/DF
3×10^{-3}	18.28[b]	11.07 (0.043)	20
1×10^{-3}	18.57 (0.066)	11.13 (0.12)	3.3
3×10^{-4}	18.02 (0.17)	11.5 (0.12)	4.2
Weighted average	18.28	11.17	

Tungstate

Total Fe (M)	log K_{C3}^{INT}	log K_{C4}^{INT}	WSOS/DF
3×10^{-3}	19.35[b]	14.23 (0.034)	1.7
1×10^{-3}	19.35[b]	13.97 (0.040)	1.4
3×10^{-4}	19.35 (0.13)	13.88 (0.080)	2.0
Weighted average	19.35	14.07	

Phosphate

Total Fe (M)	log K_{C5}^{INT}	log K_{C6}^{INT}	log K_{C7}^{INT}	WSOS/DF
1×10^{-3}	31.53 (0.15)	34.13 (1.46)	26.64 (0.30)	0.6

[a] The method of Dzombak and Morel (1990) was used to obtain error estimates and weighted averages.
[b] Fixed at this value to achieve convergence.

coverages (Fig. 2). Again, I used a combination of two surface species (D4 and D6) in the FITEQL optimisations and was able to produce a good fit to the results, with SOS/DF values of <10 for all three systems (Table 4). Of course, the optimised constants were larger than those of MoO_4^{2-}, reflecting the stronger affinity of WO_4^{2-}.

When I optimised constants for the CDM, I assumed that the CD value (i.e., the fraction of the charge of the central atom in the complex that is distributed towards the *o*-plane) for a XO_4^{2-} bidentate complex is 0.5, whereas it is 0.25 for a monodentate complex, in line with the optimal values discussed by Rietra et al. (1999). This results in the stoichiometry of the electrostatic components P_o and P_b shown in Table 2. First, it was examined whether the bidentate complexes $Fe_2O_2MoO_2$ or $Fe_2O_2WO_2$ could provide satisfactory fits to the data, either alone or in combination with a monodentate complex. However, very poor fits were obtained, particularly in the absence of the fully protonated monodentate complexes C1 and C3 (Table 2), which were found to be necessary to describe the low pH data. In fact, it was found that the best fits were obtained when the bidentate complexes were left out completely from the optimisation. Instead, it was found that a combination of the monodentate C1 and C2 complexes provided reasonable fits to the MoO_4^{2-} data (Table 5). For WO_4^{2-}, good fits were obtained with the analogous combination (C3 and C4).

For PO_4^{3-}, Dzombak and Morel's DLM constants provided a rather good fit to the data, whereas my previously estimated CDM constants (Gustafsson,

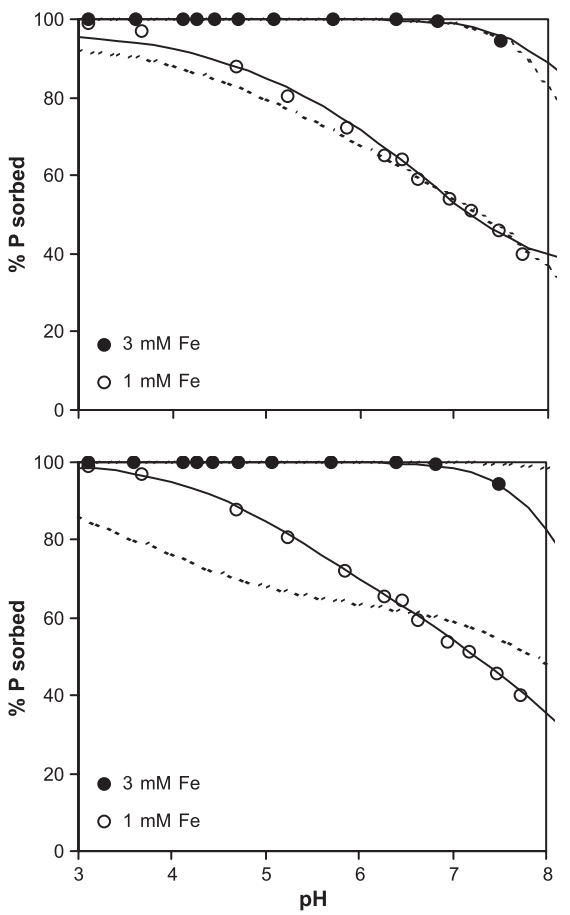

Fig. 3. Adsorption of phosphate (200 μM added) to ferrihydrite in single-sorbate systems. Points are observations, and lines are fits with the DLM (upper panel) and the CDM (lower panel). The dotted line is the model fit obtained with the non-optimized constants in Tables 1 and 2, whereas the solid line represents the fit obtained with the weighted average constants in Tables 4 and 5.

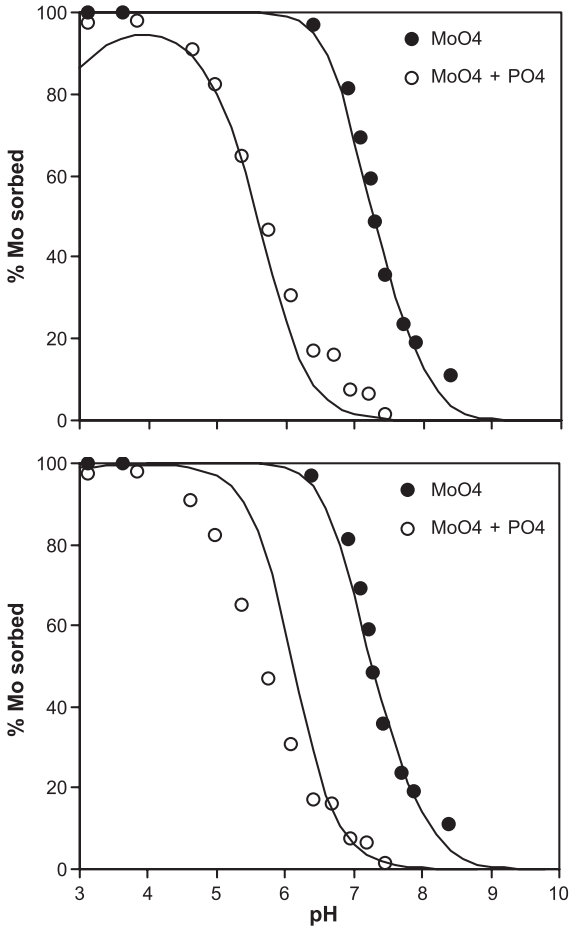

Fig. 4. Adsorption of molybdate to ferrihydrite in the presence of phosphate, at a total Fe concentration of 1×10^{-3} M. Points are observations, and lines are fits with the DLM (upper panel) and the CDM (lower panel), using the weighted average constants in Tables 4 and 5.

2001) provided a poor fit (Fig. 3). The only available data set amenable to the extraction of complexation constants by FITEQL was the one at 1 mM Fe, as almost all data at 3 mM Fe showed 100% adsorption (Table 3). For the purpose of predicting P competition effects on the adsorption of Mo and W, new constants were optimised (Tables 4 and 5), resulting in the fits shown in Fig. 3. Because I used an unrealistically large CD value for the monodentate C5 complex in my previous work (Gustafsson, 2001), it was decreased to 0.3 in this study, which would be the case if the charge of the surface oxygen in the complex is fully neutralized. In FITEQL, rather large standard deviations were obtained for the optimised PO_4^{3-} surface complexation constants (Tables 4 and 5). This indicates that the complexation constants were not fully constrained from this data set and therefore they should be regarded as crude estimates.

3.2. Competitive interactions

In the presence of 200 μM added PO_4^{3-}, the MoO_4^{2-} adsorption envelope was shifted almost 2 pH units to the left on the pH scale (Fig. 4). However, despite the strong competition from PO_4^{3-}, MoO_4^{2-}

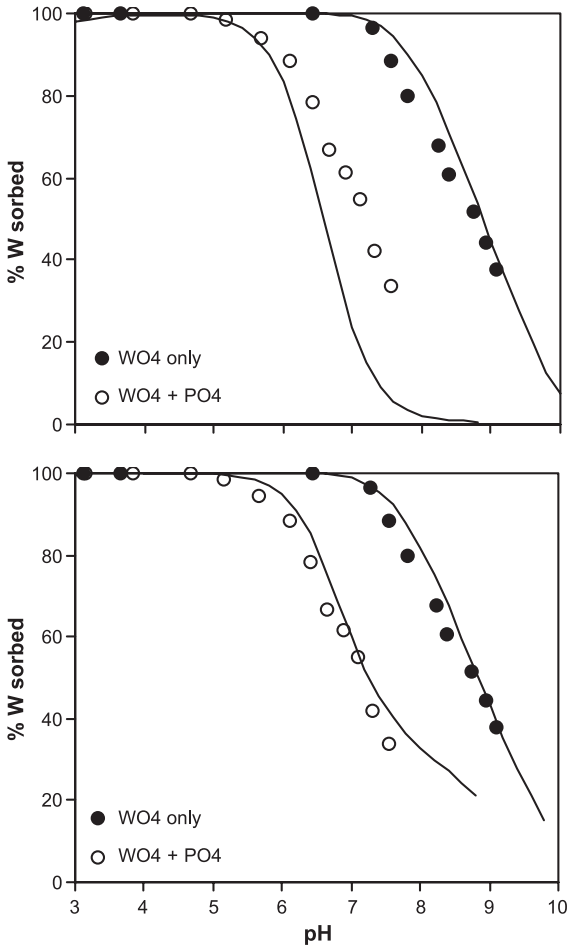

Fig. 5. Adsorption of tungstate to ferrihydrite in the presence of phosphate, at a total Fe concentration of 1×10^{-3} M. Points are observations, and lines are fits with the DLM (upper panel) and the CDM (lower panel), using the weighted average constants in Tables 4 and 5.

adsorption still approached 100% at pH < 4. With DLM, the results were simulated well, except at pH < 4.5, where DLM overestimated the dissolved MoO_4^{2-} concentration. The CDM provided a less satisfying fit, as the dissolved MoO_4^{2-} concentration was underestimated considerably below pH 6.5. For both models, it was found that the fully protonated surface species (D1 and C1) dominated the Mo surface speciation completely, whereas the less protonated species (D3 and C2) had almost disappeared because of PO_4^{3-} competition.

The $WO_4^{2-} + PO_4^{3-}$ system displayed a similar behaviour, although the WO_4^{2-} ions were displaced less easily than MoO_4^{2-}, in agreement with the stronger overall adsorption of WO_4^{2-} (Fig. 5). At pH < 5.5, almost 100% was adsorbed. In this case, the DLM could not predict the WO_4^{2-} concentration satisfactorily, as adsorption was underestimated, particularly at high pH. For the CDM, however, WO_4^{2-} adsorption was predicted rather well.

Because MoO_4^{2-} and WO_4^{2-} adsorbed strongly at low pH despite the competition from PO_4^{3-}, it was not surprising that the adsorption of PO_4^{3-} was affected. As Fig. 6 implies, the presence of MoO_4^{2-} or WO_4^{2-} caused a strong effect on the dissolved PO_4^{3-} concentration. Tungstate was found to affect PO_4^{3-} adsorption the most, in agreement with the finding that WO_4^{2-} adsorbs more strongly than MoO_4^{2-}. Both models were able to simulate the effect at least in a qualitative sense, but for the DLM, there was a clear deviation at the two lowest pH values (< pH 4).

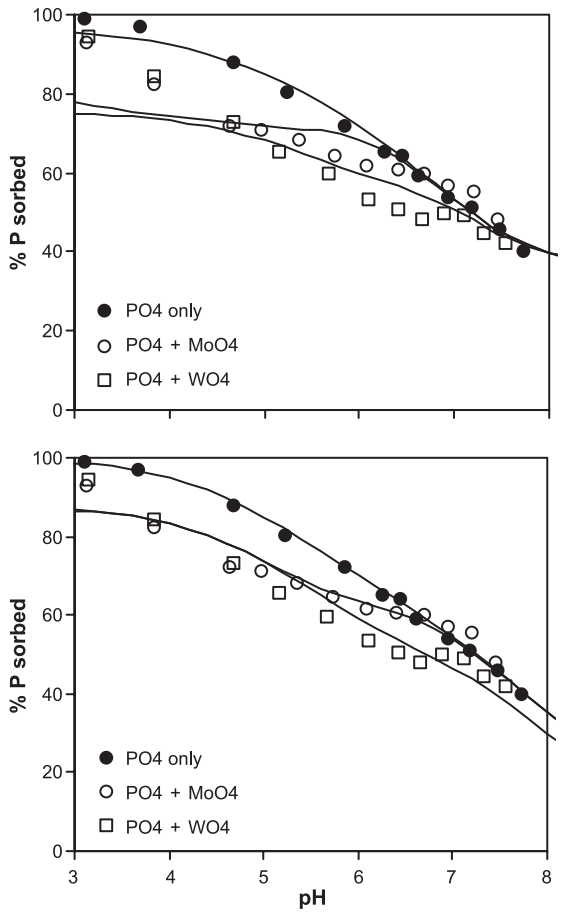

Fig. 6. Adsorption of phosphate to ferrihydrite, in the absence or presence of molybdate and tungstate), at a total Fe concentration of 1×10^{-3} M. Points are observations, and lines are fits with the DLM (upper panel) or CDM (lower panel), using the weighted average constants in Tables 4 and 5.

4. Discussion

This study suggests that the adsorption of MoO_4^{2-} and WO_4^{2-} to ferrihydrite can be described with two monodentate surface complexes in a surface complexation model. This does not rule out the existence of other surface complexes, such as the bidentate complex $Fe_2O_2XO_2$, although they seem to be less important in affecting the shape of the adsorption envelope. In competitive systems with PO_4^{3-}, the model fits were not always satisfactory. It is possible that this is mainly related to the relatively large uncertainty of the values for the PO_4^{3-} surface complexation constants. For example, slight changes in the CD values for the different PO_4^{3-} surface complexes may produce equally good fits for PO_4^{3-} in FITEQL, and substantially different fits for MoO_4^{2-} and WO_4^{2-} in competitive systems, compared to those presented here (data not shown). This shows that a more extensive data set is needed for anion binding to ferrihydrite, to constrain the surface complexation constants and to correctly predict anion competition.

In general, the DLM complexes suggested here are consistent with the CCM complexes for goethite that were proposed by Goldberg et al. (Goldberg et al., 1996; Manning and Goldberg, 1996), although they used a combination of the D1 and D2 complexes. However, the DLM constants that were predicted by

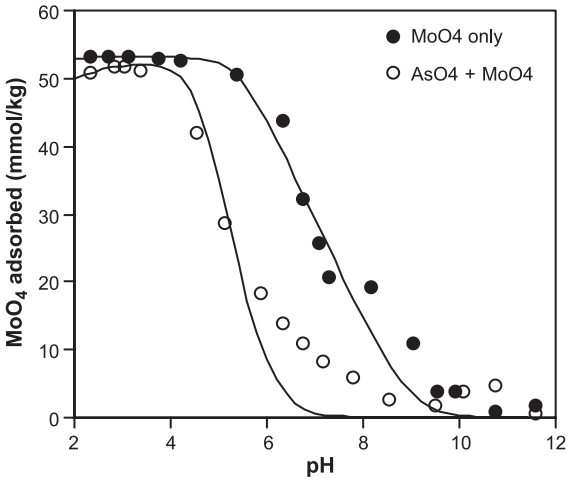

Fig. 7. Adsorption of molybdate to goethite, in the absence or presence of arsenate. The data are from Manning and Goldberg (1996). The lines are CDM fits using log $K_{C1} = 17$ and log $K_{C2} = 12$ (see text).

Dzombak and Morel (1990) using LFER proved to underestimate adsorption, particularly for WO_4^{2-}. Because Dzombak and Morel (1990) used only the first pK_a value as a basis in their LFER, part of the explanation may be the small difference between the two pK_a values for MoO_4^{2-} and WO_4^{2-}. This enables the fully protonated D1 and D4 complexes to be of importance, in conflict with the LFER results. Still, this does not explain the observation that WO_4^{2-} adsorbs much stronger than MoO_4^{2-}, as the two ions have similar pK_a values. This shows that other factors may influence the relative affinity of various surface complexes. The issue why WO_4^{2-} adsorbs so much more strongly than MoO_4^{2-} is, however, unresolved and open to speculation.

It is probable that the model approach can be extended to other Fe oxides. Manning and Goldberg (1996) presented results on the MoO_4^{2-} adsorption to goethite in single-sorbate systems and in competitive systems with AsO_4^{3-} (Fig. 7). Hiemstra and Van Riemsdijk (1999) derived surface parameters and AsO_4^{3-} constants for the application of CDM to this system. I found that MoO_4^{2-} adsorption could be described rather well if the log K's of the C1 and C2 complexes were slightly modified (to 17 and 12, respectively, see Fig. 7). Despite the smaller value of log K_{C1}, the C1 complex had to be included to simulate the AsO_4^{3-} competition in Fig. 7 correctly. Its replacement with the bidentate complex $Fe_2O_2MoO_2$ led to very poor fits at low pH (data not shown).

Despite the apparent success with the CDM proposed, it should be noted that Rietra et al.'s results on the proton coadsorption stoichiometry for the MoO_4^{2-} and WO_4^{2-} adsorption to goethite could not be accurately reproduced at pH 4.2, although it was closer to the observations at pH 6.1. Whereas the measured proton stoichiometry was ~ 1.24 at pH 4.2 after the addition of 0.8 mM Na_2MoO_4, the simulated stoichiometry with my model was 1.08. For pH 6.1, the figures were 1.42 and 1.33, respectively. Possibly, the discrepancy may, after all, be explained if the $Fe_2O_2MoO_2$ complex is present as an additional complex that is of some importance at low pH.

5. Conclusions

This study demonstrates that the adsorption of WO_4^{2-} to ferrihydrite is stronger than that of MoO_4^{2-}. The adsorption of these anions can be described by two monodentate surface complexes in both the DLM and the CDM. Molybdate and tungstate were adsorbed very strongly at low pH, where the ions were able to displace PO_4^{3-} from the ferrihydrite surface. This could be explained only if the model considers the presence of a fully protonated complex, equivalent to molybdic or tungstic acid adsorbed onto the oxide surface. The same observation was made for a system with goethite. These results are of importance for assessments of Mo and W mobility in the environment.

Acknowledgements

The Geological Survey of Sweden (SGU) and the Swedish Research Council (VR) provided financial support to this study. Björn Evertsson is acknowledged for assistance with Mo and W analyses. **[EO]**

References

Balistrieri, L.S., Chao, T.T., 1990. Adsorption of selenium by amorphous iron oxyhydroxide and manganese dioxide. Geochim. Cosmochim. Acta 54, 739–751.

Bibak, A., Borggaard, O.K., 1994. Molybdenum adsorption by aluminium and iron oxides and humic acid. Soil Sci. 158, 323–327.

Bourikas, K., Hiemstra, T., Van Riemsdijk, W.H., 2001. Adsorption of molybdate monomers and polymers on titania with a multisite approach. J. Phys. Chem. B 105, 2393–2403.

Clausen, L., Fabricius, I., 2000. BET measurements: outgassing of minerals. J. Colloid Interface Sci. 227, 7–15.

Cruywagen, J.J., 2000. Protonation, oligomerization, and condensation reactions of vanadate(V), molybdate(VI), and tungstate (VI). Adv. Inorg. Chem. 49, 127–182.

Cruywagen, J.J., Rohwer, E.A., Wessels, G.F.S., 1995. Molybdenum(VI) complex formation: 8. Equilibria and thermodynamic quantities for the reactions with citrate. Polyhedron 14, 3481–3493.

Dzombak, D.A., Morel, F.M.M., 1990. Surface Complexation Modeling—Hydrous Ferric Oxide. Wiley, New York.

Goldberg, S., Forster, H.S., 1998. Factors affecting molybdenum adsorption by soils and minerals. Soil Sci. 163, 109–114.

Goldberg, S., Forster, H.S., Godfrey, C.L., 1996. Molybdenum adsorption on oxides, clay minerals, and soils. Soil Sci. Soc. Am. J. 60, 425–432.

Gustafsson, J.P., 2001. Modelling competitive anion adsorption on oxide minerals and an allophane-containing soil. Eur. J. Soil Sci. 52, 639–653.

Herbelin, A.L., Westall, J.C., 1999. FITEQL 4.0: A Computer Program for Determination of Chemical Equilibrium Constants from Experimental Data; Report 99-01. Department of Chemistry, Oregon State University, Corvallis.

Hiemstra, T., Van Riemsdijk, W.H., 1996. A surface structural approach to ion adsorption: the charge distribution (CD) model. J. Colloid Interface Sci. 179, 448–508.

Hiemstra, T., Van Riemsdijk, W.H., 1999. Surface structural ion adsorption modeling of competitive binding of oxyanions by metal (hydr)oxides. J. Colloid Interface Sci. 210, 182–193.

Jacks, G., 1983. Undersökning av askprofiler från Nottingham, England. KHM Teknisk Rapport, vol. 104. Vattenfall, Stockholm, Sweden. In Swedish.

Manning, B.A., Goldberg, S., 1996. Modelling competitive adsorption of arsenate with phosphate and molybdate on oxide minerals. Soil Sci. Soc. Am. J. 60, 121–131.

Meima, J.A., van der Weijden, R.D., Eighmy, T.T., Comans, R.N.J., 2002. Carbonation processes in municipal solid waste incinerator bottom ash and their effect on the leaching of copper and molybdenum. Appl. Geochem. 17, 1503–1513.

Mikkonen, A., Tummavuori, J., 1993. Retention of tungsten(VI) by three Finnish mineral soils. Acta Agric. Scand., B Soil Plant Sci. 43, 213–217.

Mikkonen, A., Tummavuori, J., 1994. Desorption of phosphate from three Finnish mineral soil samples during adsorption of vanadate, molybdate and tungstate. Agric. Sci. Finl. 3, 481–486.

Rietra, R.P.J.J., Hiemstra, T., Van Riemsdijk, W.H., 1999. The relationship between molecular structure and ion adsorption on variable charge minerals. Geochim. Cosmochim. Acta 63, 3009–3015.

Schwertmann, U., Cornell, R.M., 2000. Iron Oxides in the Laboratory. Preparation and Characterization. Wiley, Weinheim.

Smith, R.M., Martell, A.E., Motekaitis, R.J., 2001. NIST Critically Selected Stability Constants of Metal Complexes Database. Version 6.0. NIST Standard Reference Database, vol. 46. National Institute of Standards and Technology, US Department of Commerce, Gaithersburg.

Swedlund, P.J., Webster, J.G., 1999. Adsorption and polymerisation of silicic acid on ferrihydrite, and its effect on arsenic adsorption. Water Res. 33, 3413–3422.

Vunkova-Radeva, R., Schiemann, J., Mendel, R.R., Salcheva, G., Georgieva, D., 1988. Stress and activity of molybdenum-containing complex in winter wheat seeds. Plant Physiol. 87, 533–535.

Wesolowski, D., Drummond, S.E., Mesmer, R.E., Ohmoto, H., 1984. Hydrolysis equilibria of tungsten(VI) in aqueous sodium chloride solutions to 300 °C. Inorg. Chem. 23, 1120–1132.

Wood, S.A., Samson, I.M., 2000. The hydrothermal geochemistry of tungsten in granitoid environments: I. Relative solubilities of ferberite and scheelite as a function of T, P, pH and m_{NaCl}. Econ. Geol. 95, 143–182.